journal

XAFS Investigation of Platinum Impurities in Phosphate Glasses

Mevlut Karabulut,*,† G. Kanishka Marasinghe,*,‡ Carol A. Click,* EzzEldin Metwalli,*,§ and
Richard K. Brow*

Graduate Center for Materials Research, University of Missouri, Rolla, Missouri 65401

Corwin H. Booth, J. J. Bucher, and David K. Shuh

Chemical Sciences Division, Lawrence Berkeley National Laboratory, Berkeley, California 94720

Tayyab I. Suratwala* and John H. Campbell*

Lawrence Livermore National Laboratory, Livermore, California 94550

The coordination environments of Pt impurities in a ternary
K-aluminophosphate (KAP) glass and commercial K,Mg-
aluminophosphate (KMAP) laser glasses have been investi-
gated by Pt L_{III}-edge X-ray absorption fine structure (XAFS)
spectroscopy. Pt valence in the KAP glass depends on the melt
preparation atmosphere. Pt^{4+} ions form in melts that are
bubbled with oxygen, whereas metallic Pt particles form when
these same samples are remelted in air. Residual chlorine in
KMAP glasses has an effect on Pt bonding. In chlorine-free
samples, Pt^{4+} ions are coordinated with ~5.4 (8) oxygen atoms
with an average distance of 2.02 (1) Å. For glasses with low
chlorine contents (<200 ppm Cl), the Pt^{4+} ions have both O
and Cl atoms in the first coordination shell. As the Cl
concentration increases, the number of O nearest neighbors
decreases and for Cl:Pt > 5, only Cl nearest neighbors are
observed. Pt^{4+} ions in these latter glasses are coordinated by
~5.5 (8) Cl atoms at an average distance of 2.27 (2) Å.

I. Introduction

PHOSPHATE glasses are widely used as rare-earth host materials
for solid-state lasers. These glasses can be produced in large
sizes with high optical homogeneity and the composition of the
host glass can be tailored for specific laser applications.[1] Nd-doped
phosphate glasses have excellent laser and optical properties[1,2] and
are the materials of choice for high-energy/high-peak-power la-
sers.[3] The production of high-optical-quality, high-purity compo-
sitions is critical for these applications.

It is standard practice to melt phosphate laser glasses in
platinum containers to produce high-quality, homogeneous optical
glasses, despite the incorporation of Pt impurities.[4] Platinum
dissolves into glass melts, either as ionic platinum or as metallic Pt
inclusions. Pt dissolution occurs by a variety of mechanisms
including vapor-phase transport of platinum compounds from the
crucible above the melt surface, mechanical abrasion of platinum
surfaces, and reaction with the melting batch.[5,6] One advantage of
phosphate glass for use as a high-power laser host, compared with
silicate or fluorophosphate laser glasses, is the high solubility of
platinum ions which reduces the risk of the formation of metallic
platinum inclusions.[6] Platinum metal inclusions can initiate cata-
strophic damage to glasses used in high-power laser applications.
Inclusions in glasses irradiated above the threshold laser fluence
will heat until they volatilize and fracture the laser glass.[7] In
contrast, dissolved platinum ions (Pt^{4+}) have negligible impact on
the laser performance of the glass except for a small drop in
pumping efficiency.[5]

Previous studies of platinum dissolution in phosphate laser
glasses have mainly focused on the platinum dissolution process-
es.[5–7] Platinum ions are dissolved into phosphate melts under
oxidizing conditions, whereas metallic Pt inclusions form under
reducing conditions.[7] Pt^{4+} ions absorb near 400 nm, giving
phosphate glasses a yellow color; metallic platinum inclusions
impart a gray color to phosphate glasses.[8] The oxidizing conditions
favoring Pt dissolution can be achieved by using O_2, Cl_2, or other
Cl-containing gases (e.g., $POCl_3$, CCl_4). A combination of O_2/Cl_2
is often used in commercial melting operations.[9]

Little is known about the local chemical environment of
platinum ions in phosphate glasses. Recently, the coordination
environments of Pt ions in silicate glasses were investigated by Pt
L_{III}-edge X-ray absorption fine structure (XAFS) spectroscopy.[10]
It was found that the Pt ions are primarily tetravalent and
octahedrally coordinated by O with a mean Pt–O distance of
2.08 Å.

In the present study, we have used Pt L_{III}-edge XAFS to
investigate the local environment of Pt impurities in several
phosphate glasses, including a commercial laser composition
melted under O_2 and O_2 + Cl_2 process gas environments. The
XAFS data are compared with data collected from model com-
pounds to determine the Pt oxidation state, coordination number,
and nearest-neighbor anions (O^{2-} versus Cl^-).

II. Experimental Details

(1) Glass Preparation

Three sets of Pt-containing phosphate glasses were examined in
this study. The first set includes two samples of a ternary metaphos-
phate glass with the nominal composition $40K_2O \cdot 5Al_2O_3 \cdot 55P_2O_5$

(mol%), denoted KAP-1. The glass was prepared from mixtures of $K_2HPO_4\cdot3H_2O$, $Al(PO_3)_3$, and $NH_4H_2PO_4$ melted in a silica crucible for 1 h at 900°C, then quenched on steel plates to form a clear glass. A 30 mL portion of glass was then remelted in a silica crucible at 1100°C. A platinum metal strip with a surface area of 26 mm^2 was submerged into the bubble-free, homogeneous melt and then the melt was bubbled with oxygen at a flow rate of ~1 L/min for 9 h. The platinum strip was then removed from the crucible and about one-half of the melt was quenched and annealed at 300°C to form a Pt-containing glass, denoted KAP-1Y. This glass had a characteristic yellow color resulting from absorption by Pt^{4+} ions.[8] (The optical spectra of Pt^{4+} containing glasses are described elsewhere.[11]) The remaining melt was returned to the 1100°C furnace for an additional 5 h to equilibrate with air. On quenching and annealing (again at 300°C), the remaining melt produced a gray glass, denoted KAP-1G. Both KAP-1Y and KAP-1G contain ~280 ppm of Pt, as estimated from the Pt strip weight loss.

A second set of samples was prepared using the commercial phosphate laser glass LG-770[6] as the starting material. LG-770 has the approximate composition $(20–25)K_2O\cdot(5–10)MgO\cdot(6–10)Al_2O_3\cdot(58–62)P_2O_5$ (mol%) and was doped with 4.2×10^{20} Nd ions/cm^3.[3] The glass was prepared using a melting technique described elsewhere.[9] The experimental samples were prepared by melting glass in a Pt crucible at 1100°C and bubbling either O_2 or O_2/Cl_2 gas mixtures through the melts for times varying from a few hours to several days to achieve a range of Pt^{4+} and Cl$^-$ concentrations. These samples are denoted "KMAP". Annealed glasses from these melts were analyzed by inductively coupled plasma/atomic emission spectrometry (ICP/AES) to verify that the base composition had not changed during the course of melting. The Pt concentration was also determined by ICP/AES and the Cl content was determined using X-ray fluorescence. NIST traceable standards were used to calibrate the analytical measurements. Table I lists the Pt and Cl concentrations in the KMAP samples.

(2) XAFS Data Collection

Room-temperature Pt L_{III}-edge XAFS spectra were collected at the Stanford Synchrotron Radiation Laboratory (SSRL) on beamline 4-1 using a half-tuned Si(220) double-crystal monochromator. Powders (~75 μm) from each glass were mixed with polystyrene beads. All spectra were collected in fluorescence mode using a Ge solid-state detector.[12] Because of the low Pt content in the glasses, in general, 8 to 12 scans to $k = 13$ Å^{-1} were averaged for each sample to improve the signal-to-noise ratio. All spectra were energy calibrated by simultaneously measuring the absorption spectrum from a Pt reference foil. XAFS spectra were also collected from two model compounds, PtO_2 and H_2PtCl_6. These, along with the Pt foil, are used as references for the Pt valence states and coordination environments in glasses with and without Cl.

(3) Theory and Data Analysis

The primary X-ray absorption edge is due to the dipole transitions caused by the excitation of core photoelectrons into
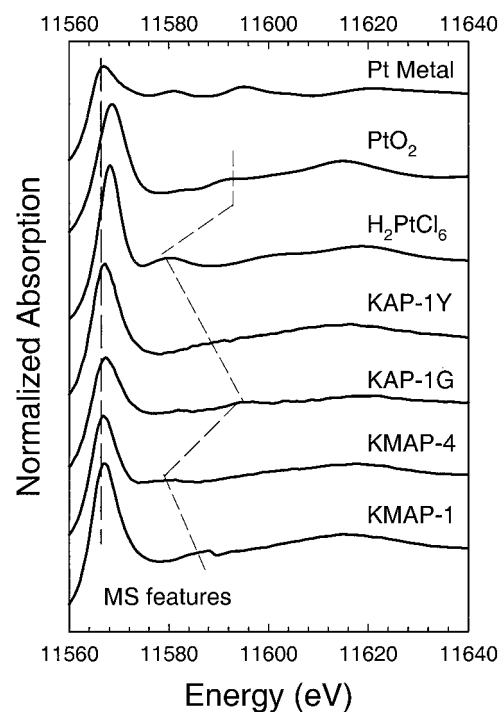

Fig. 1. Normalized Pt L_{III}-edge XANES spectra for selected glasses along with spectra from two Pt^{4+} reference compounds (PtO_2 and H_2PtCl_6) and metallic Pt. The features indicated by dotted lines are due to the multiple scattering (MS).

empty states above the Fermi level (for example, $2p$–$5d$ for the Pt L_{III}-edge). Spectra from the region extending up to 50 eV above the main edge are known as the X-ray absorption near-edge structure (XANES). The effects of multiple scattering of photoelectrons with moderate kinetic energy by surrounding atoms must be accounted for to interpret these spectra.[13]

Energy calibration was done by setting the first derivative of the L_{III}-edge of the Pt metal foil to 11564 eV. The calibration is good to about 0.1 eV or even better, but the edge positions for the other samples are worse, around 0.3 eV, partially due to the noise in the data and also because the edge shapes are more complicated. After a linear pre-edge background was removed, the XANES spectra were normalized to a step height of 1.

Spectra obtained from the region extending from the XANES region to as high as 2 keV above the edge are known as the extended X-ray absorption fine structure (EXAFS), and are primarily due to the scattering of the photoelectron off near-neighbor atoms. The amplitude of the EXAFS function $\chi(k)$ where k is the wave vector, is proportional to the number of nearest neighbors, and the change of phase with the wavelength of the photoelectron depends on the distance between the emitter and the backscattering atom.[13–15] The backscattering strength also depends on the type or atomic number of atoms involved in the backscattering process. Thus, an analysis of EXAFS data yields structural details about the absorbing atom and its local structural environment.

EXAFS data reduction was conducted by standard methods described elsewhere[13–15] using the suite of programs EXAFSPAK. The background was removed by fitting the pre-edge with a polynomial function such that the background-subtracted absorption above the edge follows the Victoreen formula. The EXAFS oscillations were isolated from the central atom absorption using a spline function. The energies then were recalculated into k-space using $k = [2m(E - E_0)]^{1/2}/\hbar$. The EXAFS threshold energy, E_0 (energy where the momentum (k) is zero), was defined as 11580 eV for all of the glasses for the purposes of the fits. The raw EXAFS spectra were fitted in the 2–11 Å^{-1} range using theoretical backscattering phase and amplitude functions for the appropriate scattering paths. The backscattering O and Cl amplitudes and Pt–O and Pt–Cl phase shifts were calculated from the crystalline PtO_2

Table I. Pt and Cl Contents in the Glasses Investigated

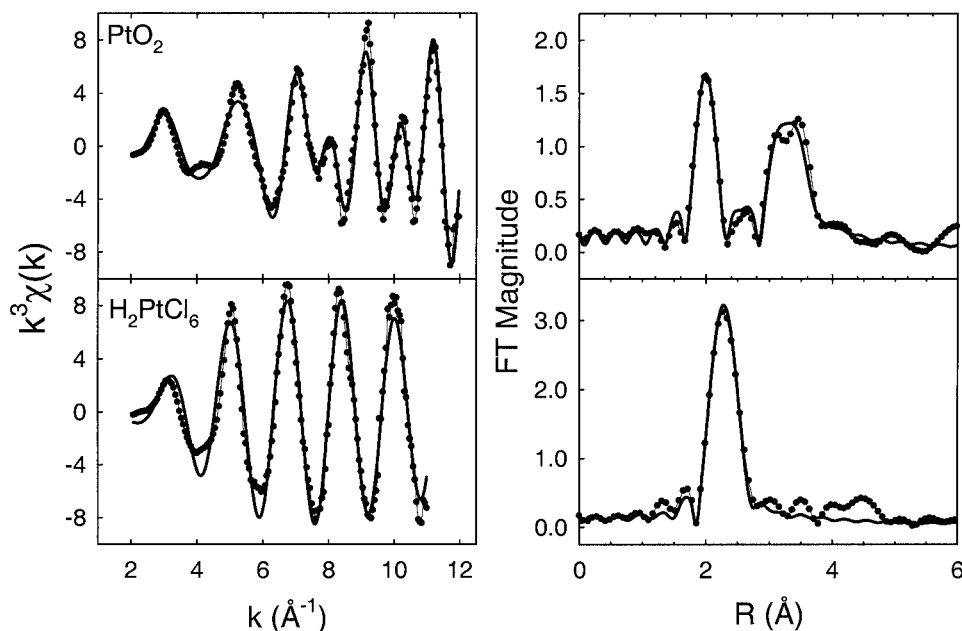| Glass	Process gas	Pt (ppm wt)	Cl (ppm wt)	Atom ratio Cl:Pt
KAP-1Y	O_2	280		
KAP-1G	Air	280		
KMAP-1	O_2	552		
KMAP-2	O_2	248		
KMAP-3	O_2	187		
KMAP-4	O_2/Cl_2	670	734	6.03
KMAP-5	O_2/Cl_2	604	538	4.90
KMAP-6	O_2/Cl_2	644	378	3.23
KMAP-7	O_2/Cl_2	765	240	1.73
KMAP-8	O_2/Cl_2	934	228	1.34
KMAP-9	O_2/Cl_2	644	140	1.20

Fig. 2. k^3-weighted EXAFS spectra (left) and corresponding Fourier transforms (FT, uncorrected for phase shift) for the two reference compounds PtO_2 and H_2PtCl_6. The dotted lines indicate the experimental data and the solid lines represent the theoretical fits.

and $PtCl_4$ phases using the FEFF7 multiple scattering code.[16] An overall amplitude reduction factor, $S_0^2 = 0.8$, was obtained by fixing the number of O neighbors in the fits to the PtO_2 data to a nominal value of 6, and this amplitude reduction factor was used in all subsequent fits.

III. Results

(1) XANES Measurements

The Pt L_{III}-edge XANES spectra for selected glasses and Pt model compounds (PtO_2 and H_2PtCl_6) together with Pt metal are given in Fig. 1. The main absorption edge position of PtO_2 is ~1.7 (3) eV above the metal's edge and the absorption edge of H_2PtCl_6 is 1.5 (3) eV above the metal's edge. Edge positions of all the

glasses are around 0.3 (2) eV above the metal except for the KMAP-2 glass, for which the shift is around 0.6 (3) eV.

In addition to the main absorption edges, there is another feature observed at ~12 and ~24 eV above the edge in the XANES spectrum of H_2PtCl_6 and PtO_2, respectively. Even though much less pronounced, this feature is also observed in the XANES spectra of the phosphate glasses. Similar features were observed in a previous XAFS investigation of Pt incorporated into in silicate glasses.[10] It is interesting to note that this secondary feature is observed at the same energy for the KMAP-4 sample, with 734 ppm Cl, and for H_2PtCl_6, indicating that Pt ions have similar coordination environments in both samples. *Ab initio* XANES calculations on PtO_6 and $PtCl_6$ clusters showed that this high-energy feature is due to the multiple scattering (O–Pt–O and
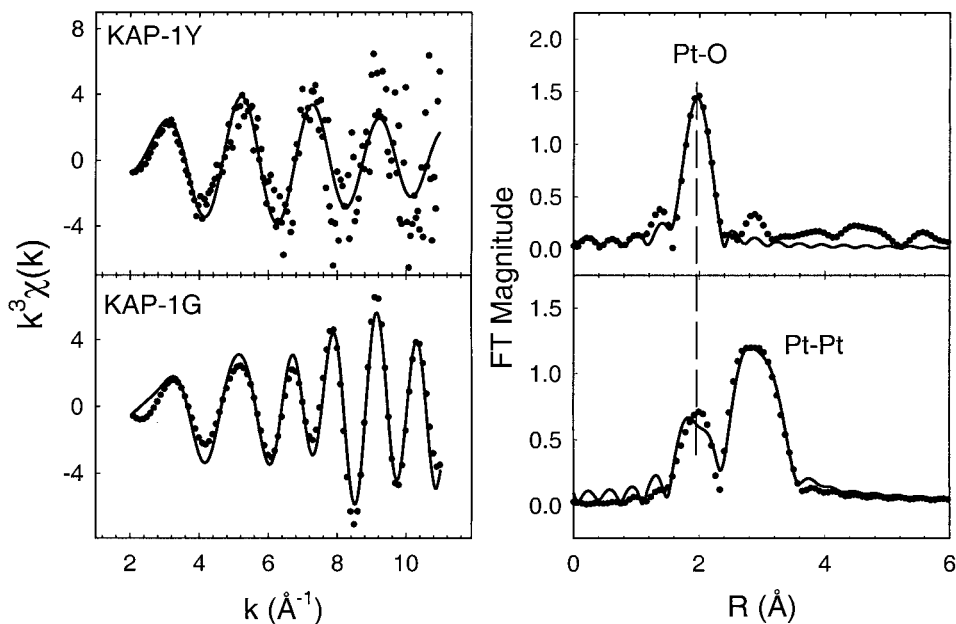

Fig. 3. k^3-weighted EXAFS spectra (left) and corresponding FTs (right) for the KAP-1Y and KAP-1G glasses. Fourier filtered (1–4 Å) data were fitted for the KAP-1G glass. The fit range is from 2 to 11 Å^{-1}. The dotted lines indicate the experimental data and the solid lines represent the theoretical fits.

Table II. Structural Parameters for KAP-1 Glasses Obtained from Pt L_{III}-edge EXAFS Fits[†]

	Pt–O Shell			Pt–Pt Shell		
Glass	N	R (Å)	σ (Å)	N	R (Å)	σ (Å)
KAP-1Y	5.5 (9)	2.00 (2)	0.05 (2)			
KAP-1G	2.4 (6)	1.99 (1)	0.07 (2)	8.4 (10)	2.76 (2)	0.08 (2)

[†]N is the number of nearest neighbors in a shell, R is the average interatomic distance for a given shell, and σ is the EXAFS Debye–Waller factor. The errors given in parentheses give the 95% confidence limits calculated by EXAFSPAK. An overall amplitude reduction factor $S_0^2 = 0.8$ was used for all of the Pt L_{III}-edge EXAFS fits in this study. Fourier filtered data (1–4 Å) were fitted for the KAP-1G glass.

Cl–Pt–Cl) of the ejected photoelectrons.[10] In a recent Pt L_{III}-edge XANES study of Pt–Cl systems, some of the postedge XANES features were assigned to hybridization peaks mediated by multiple scattering.[17] The effective length of this multiple scattering path is larger for $PtCl_6$ compared with PtO_6 due to the larger ionic radius of Cl^- (~1.7 Å) compared with O^{2-} (~1.4 Å). Longer Pt–Cl bonds and hybridization effects shift the position of the multiple scattering-related feature to lower energies in glasses containing Cl.[10,18,19]

(2) EXAFS Measurements

Figure 2 shows the k^3-weighted EXAFS and corresponding Fourier transforms (FT) for PtO_2 and H_2PtCl_6 (uncorrected for the phase shifts of the photoelectron wave). The fits are given as solid lines and the experimental data as the dotted lines. (The same convention is used in all subsequent spectra.) The FT obtained from EXAFS is similar to a radial distribution function, but shows only the peaks involving the central absorbing atom. EXAFS fits reveal that the first peak observed in the FT of PtO_2 is due to the oxygen neighbors around Pt ions with an average Pt–O distance of 2.02 (1) Å. In the structure of crystalline PtO_2, there are six oxygen neighbors around Pt, four of them are at 1.98 Å and two of them

are at 2.02 Å.[19] The second peak in the PtO_2 FT in Fig. 2 is due to the Pt–Pt scattering path with an average distance of 3.1 (2) Å, consistent with the reported structure of crystalline PtO_2.[19] The FT of H_2PtCl_6 has a single peak due to 5.6 (3) Cl neighbors around Pt at an average distance of 2.32 (1) Å. These distances are in agreement with the Pt–Cl distances obtained from X-ray diffraction measurements of $PtCl_6^{2-}$ moieties in Pt-chloride compounds.[20,21]

Figure 3 shows the k^3-weighted EXAFS and corresponding FTs for the KAP-1Y and KAP-1G glasses. The KAP-1G data were noisier than the KAP-1Y data and the fit for the KAP-1G sample was done using Fourier filtered data (1–4 Å with a Gaussian width of 0.3 Å). Raw EXAFS data were fitted for all of the other glasses. As shown in Fig. 3, the EXAFS spectra and FTs of these two glasses are quite different. As described above, the KAP glasses have the same base composition and the same Pt contents but were melted under different conditions. The structural parameters obtained from the EXAFS fits are summarized in Table II. In the spectrum of KAP-1Y glass, the only resolvable contribution is due to the Pt–O scattering path which is centered at 2.00 (2) Å with a coordination number of 5.5 (9). In the spectrum of KAP-1G glass, the main contribution is due not to the Pt(IV)–O scattering, which is still observed at 1.99 (1) Å, but instead comes from Pt–Pt scattering characteristic of Pt metal, observed at a distance of 2.76 (2) Å with a coordination number of 8.4 (10). Diffraction studies of Pt metal indicate that each Pt atom has 12 other Pt atoms in the first coordination shell with an average Pt–Pt distance of 2.78 Å.[22]

Figure 4 shows the k^3-weighted EXAFS spectra and corresponding FTs for the chlorine-free KMAP glasses. These glasses each have the same base composition but contain different amounts of Pt impurities. The structural parameters are summarized in Table III. Only the first nearest neighbors can be resolved from the fits. There is no discernible dependence of the Pt local environments on Pt concentration. The Pt^{4+} ions have ~5.4 (8) oxygen nearest neighbors at an average distance of 2.02 (1) Å, similar to that found for the KAP-1Y sample (Table II).

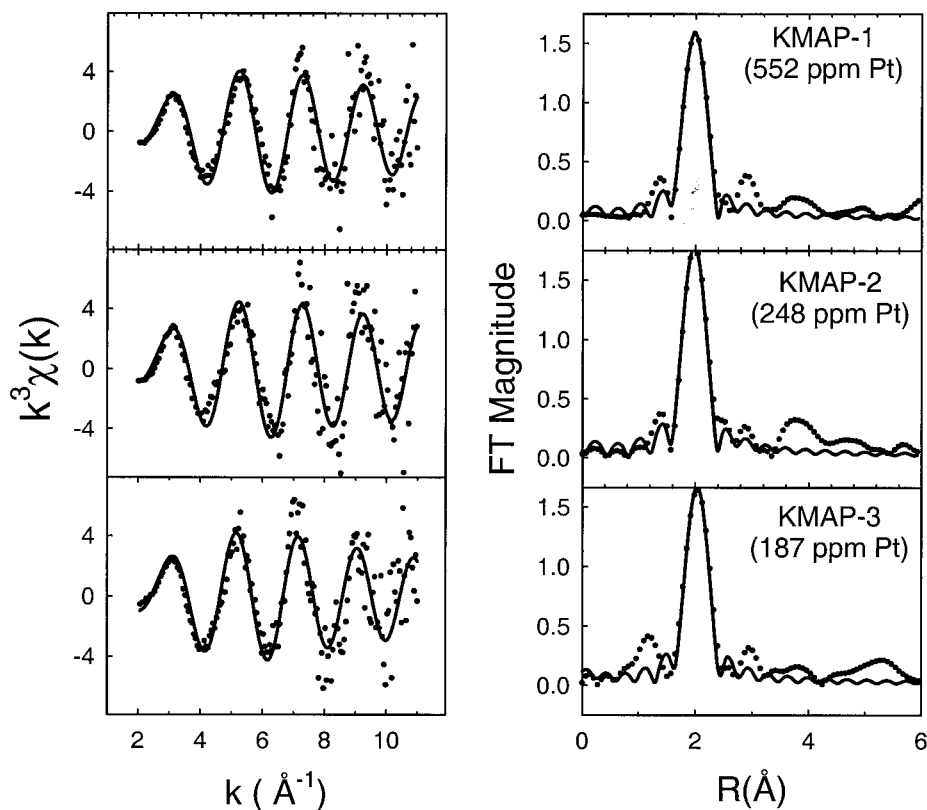**Fig. 4.** k^3-weighted EXAFS spectra (left) and corresponding FTs (right) for the KMAP glasses without Cl. The fit range is from 2 to 11 Å^{-1}. The dotted lines indicate the experimental data and the solid lines represent the theoretical fits.

Table III.　Structural Parameters for KMAP Glasses (without Cl) Obtained from Pt L_{III}-edge EXAFS Fits[†]

		Pt–O Shell	
Glass	N	R (Å)	σ (Å)
KMAP-1	5.3 (9)	2.01 (1)	0.06 (2)
KMAP-2	5.6 (6)	2.04 (1)	0.06 (2)
KAMP-3	5.5 (7)	2.01 (2)	0.05 (2)

[†]The errors given in parentheses are 95% confidence limits calculated by EXAFSPAK.

The k^3-weighted EXAFS spectra and corresponding FTs together with the theoretical fits for selected chlorine-containing KMAP glasses are shown in Fig. 5. The structural parameters obtained from the EXAFS fits are summarized in Table IV. The Debye–Waller parameter (σ) determined for the Pt–O coordination shell in the EXAFS fits of Cl-free glasses was used as a fixed parameter ($\sigma = 0.06$ Å) when fitting the EXAFS spectra of Cl-containing glasses to compare structural parameters related to the Pt–Cl coordination. The position of the first feature in the FT shifts to a longer distance as the Cl concentration in the glass increases. The shift in the position of this feature continues until the atomic Cl:Pt ratio reaches ~5. Further increases in the Cl concentration do not affect the position of this peak.

The simulations of the EXAFS spectra indicate that at low Cl concentrations, Pt ions have both O and Cl atoms as the first nearest neighbors and the relative fraction of oxygen nearest neighbors decreases with increasing Cl concentration. For the KMAP-9 sample, which contains 140 ppm Cl and 644 ppm Pt, there are on average 2.6 (6) O atoms for each Pt^{4+} at an average distance of 1.99 (2) Å and there are 2.0 (7) Cl atoms at an average distance of 2.19 (2) Å. For the KMAP-5 sample, which contains 538 ppm Cl and 604 ppm Pt, no O nearest neighbors to Pt are

observed. The sole contribution to the Pt EXAFS spectrum comes from Pt–Cl coordination centered at 2.26 (2) Å with a coordination number of 5.5 (8).

IV.　Discussion

(1)　Pt Oxidation State

The main edge positions of all the glasses coincide with each other (0.3 (2) eV above the metal edge) except the KMAP-2 sample, with an edge position that is 0.6 (3) eV above the metal edge. Compared with Pt L_{III}-edge positions of PtO_2 and H_2PtCl_6 which are 1.7 (3) eV and 1.5 (3) eV above the metal edge, respectively, the main edges of the glasses are close to the metal edge. Because of the small shifts in the Pt L_{III}-edge positions, it is difficult to draw conclusions from the XANES spectra about differences in Pt oxidation states. However, the characteristic colors of Pt^{4+} (yellow) and Pt metal (gray) in phosphate glass[8] indicate that the KAP1-G glass has a significant concentration of Pt metal inclusions and that Pt^{4+} is present in all other samples

Previous studies indicate that the redox conditions of an experiment affect how platinum is incorporated into phosphate melts:[6,7]

$$Pt + O_{2(g)} \leftrightarrow Pt^{4+}_{(glass)} + 2O^{2-} \tag{1}$$

Under oxidizing conditions, such as those used during the formation of KAP-1Y, the reaction favors Pt^{4+} formation. The EXAFS data for KAP-1Y (Fig. 3) indicate that only Pt atoms with oxygen nearest neighbors are present in the sample, expected if the Pt redox equilibrium reaction for melts processed with oxygen gas is shifted far to the right. Under neutral or reducing conditions, Pt metal is favored, as in KAP-1G. The EXAFS data for the KAP-1G glass (Fig. 3) clearly indicate the presence of metallic Pt. The FT of KAP-1G glass is dominated by the Pt–Pt peak observed at 2.76
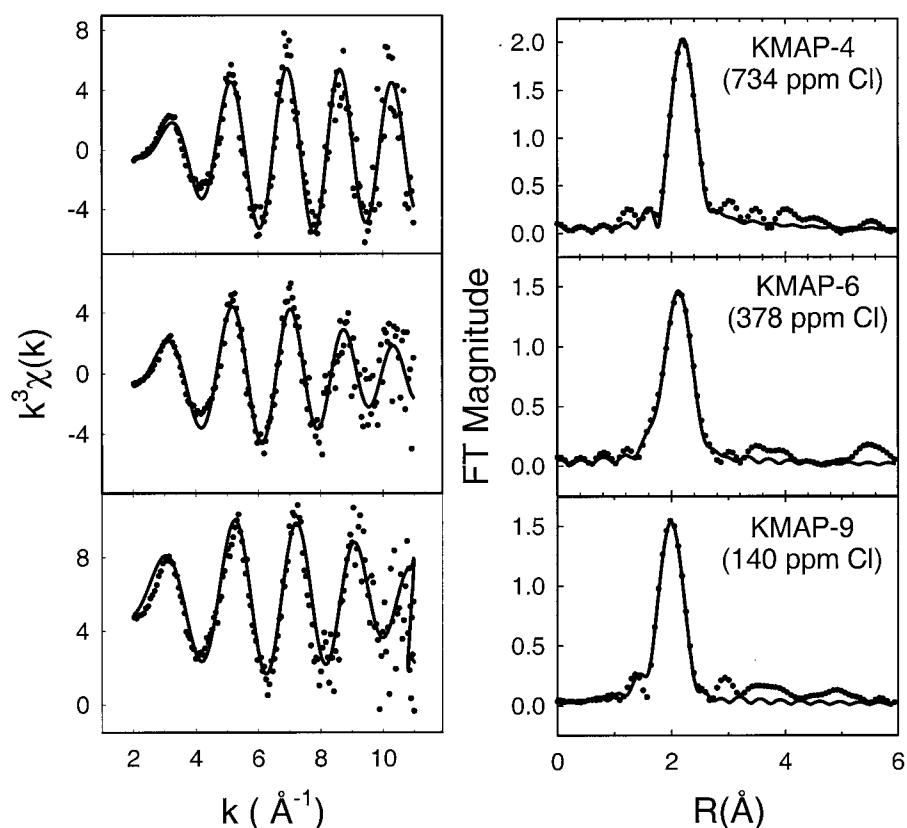

Fig. 5. k^3-weighted EXAFS spectra (left) and corresponding FTs (right) for the KMAP glasses with varying Cl⁻ content. The Pt^{4+} content is nearly constant in these glasses (~650 ppm, see Table I). The fit range is from 2 to 11 Å⁻¹. The dotted lines indicate the experimental data and the solid lines represent the theoretical fits.

Table IV. Structural Parameters for KMAP Glasses (with Cl) Obtained from Pt L_{III}-edge EXAFS Fits[†]

	Glass		Pt–O Shell			Pt–Cl Shell		
	Pt (ppm)	Cl (ppm)	N	R (Å)	σ (Å)	N	R (Å)	σ (Å)
KMAP-9	644	140	2.6 (6)	1.99 (2)	0.06	2.0 (7)	2.19 (2)	0.08
KMAP-7	765	240	2.0 (7)	2.05 (2)	0.06	2.7 (8)	2.20 (2)	0.08
KMAP-8	934	228	2.5 (6)	2.00 (2)	0.06	2.2 (4)	2.18 (2)	0.08
KMAP-6	644	378	1.0 (3)	1.96 (2)	0.06	4.0 (6)	2.24 (2)	0.08
KMAP-5	604	538				5.4 (9)	2.26 (1)	0.08
KMAP-4	670	734				5.6 (6)	2.27 (2)	0.08

[†]The errors given in parentheses are 95% confidence limits calculated by EXAFSPAK.

(2) Å, which is characteristic of metallic Pt.[10] The presence of significant contributions of Pt–O and Pt–Pt nearest neighbors to the KAP-1G spectrum indicates that both ionic Pt^{4+} and metallic Pt are present. When the Pt metal spectrum is scaled by about 40%, it fits the KAP-1G spectrum well after the first peak. This indicates that about 40% of the Pt atoms in this sample are present as metallic particles and the remaining 60% of atoms possess oxygen nearest neighbors.

(2) Pt Local Environment

The structural information obtained from the EXAFS fits is limited to the first shell neighbors for all of the glasses studied. For the chlorine-free KMAP glasses, this shell consists of ~5.5 (8) O atoms with an average distance of 2.01 (1) Å (Table III), indicating that the Pt^{4+} ions prefer octahedral coordination environments in these glasses. The average Pt–O distances derived from the EXAFS fits are similar to those observed in crystalline PtO_2 and in Pt-containing silicate glasses.[10,19]

The EXAFS fits of Cl-containing KMAP glasses reveal that as the Cl concentration increases, the number of Cl nearest neighbors to Pt^{4+} also increases, replacing O in the first coordination sphere (Table IV). The similarities observed in the XANES spectra (Fig. 1) of KMAP-4 glass (734 ppm Cl) and H_2PtCl_6 also supports this interpretation of the EXAFS results. Figure 6 shows the number of Cl and O neighbors around Pt^{4+} ions in the KMAP glasses as a function of the Cl:Pt atomic ratio. Chlorine replaces oxygen in the first coordination sphere of the Pt^{4+} ions and for glasses with Cl:Pt > 5, there are no detectable oxygen nearest neighbors. The maximum average number of Cl nearest neighbors to Pt^{4+} is 5.6 (6), indicating that $(PtCl_6)^{2-}$ moieties are present in glasses with the highest Cl^- concentrations. The Pt–Cl distance (2.26 Å) derived from the EXAFS fits is consistent with the observed distances in crystalline $PtCl_4$ (2.26 Å[20]) and K_2PtCl_6 (2.31 Å[21]).

Our observation of the preferential bonding of Cl to Pt^{4+} in these glasses is similar to observations made from other studies. In solutions, Pt^{4+} ions prefer bonds to ligands of high polarizability[23] and so favor the larger size and lower electronegativity of Cl^- ions over O^{2-} as nearest neighbors. Paul and Tiwari[24] discuss the equilibrium between Pt(IV)-oxide and Pt(IV)-chloride in sodium borate melts and note that larger amounts of a Pt(IV)-chloride complex are formed with increasing amounts of residual chloride in the melt.

No structural information beyond the nearest-neighbor environments of the Pt ions in these glasses is resolved from the EXAFS data. Thermal and/or positional disorder is especially large for weakly bonded cations beyond the first coordination sphere and this may be one of the reasons why longer-range (second coordination sphere) contributions cannot be resolved. The limited k-range and the lower quality of the data at high k also contribute to the inability to resolve the higher shells. Collecting the EXAFS data at low temperatures may improve the resolution by decreasing the thermal disorder.

V. Summary

Pt^{4+} ions are incorporated into phosphate melts processed under oxidizing conditions. Metallic platinum is observed only in glass prepared from melts equilibrated in air. In chlorine-free glasses, Pt^{4+} ions are coordinated by 5.4 (8) O atoms with an average distance of 2.02 (1) Å, indicating a preference for distorted octahedral sites in the glass. When Cl is introduced into the glass, the first shell neighbors around Pt^{4+} ions are both O and Cl for low Cl concentrations, and as the Cl concentration increases, the number of Cl nearest neighbors to Pt^{4+} increases. For glasses with the greatest chlorine contents, there are 5.6 (6) Cl nearest neighbors to Pt^{4+} with an average distance of 2.26 (2) Å.
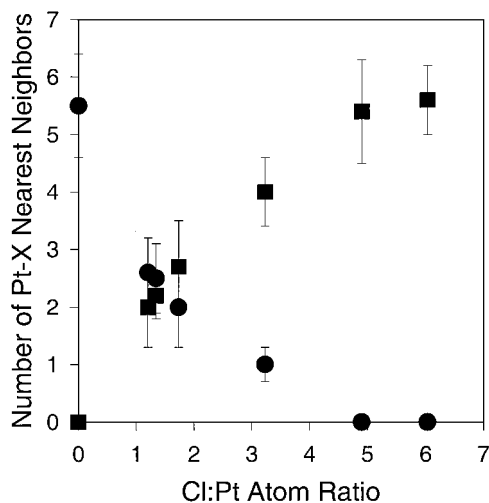
Fig. 6. Dependence of the number of O (circles) and Cl (squares) nearest neighbors around Pt ions, determined from EXAFS fits, on the Cl:Pt atomic ratio in the KMAP glasses.

References

[1]M. J. Weber, "Science and Technology of Laser Glass," *J. Non-Cryst. Solids*, **123** [1–3] 208–22 (1990).

[2]C.F. Rapp; p. 619 in *CRC Handbook of Laser Science and Technology*. Edited by M. J. Weber. CRC Press, Boca Raton, FL, 1995.

[3]J. H. Campbell and T. I. Suratwala, "Nd-Doped Phosphate Glasses for High-Energy/High-Peak-Power Lasers," *J. Non-Cryst. Solids*, **263–264**, 318–41 (2000).

[4]Y. T. Hayden, J. H. Campbell, S. A. Payne, and G. D. Wilke, "Effect of Phosphate Glass Composition on the Rate of Platinum Dissolution," *Ceram. Trans.*, **28**, 283–96 (1992).

[5]J. S. Hayden, D. L. Sapak, and A. J. Marker III, "Elimination of Metallic Platinum in Phosphate Glasses," *Proc. SPIE—Int. Soc. Opt. Eng.*, **895**, 176–81 (1988).

[6]J. H. Campbell, "Modelling Platinum-Inclusion Dissolution in Phosphate Laser Glasses," *Glastech. Ber.*, **68**, 96–101 (1995).

[7]J. H. Campbell, E. P. Wallerstein, H. Toratani, H. E. Meissner, S. Nakajima, and T. S. Izumitani, "Effects of Process Gas Environment on Platinum-Inclusion Density and Dissolution Rate in Phosphate Laser Glasses," *Glastech. Ber.*, **68** [2] 59–69 (1995).

[8]R. J. Ryder and G. E. Rindone, "Color and Light Scattering of Platinum in Some Lead Glasses," *J. Am. Ceram. Soc.*, **41** [10] 415–22 (1958).

[9]J. H. Campbell, T. I. Suratwala, C. B. Thorsness, J. S. Hayden, A. J. Thorne, J. M. Cimino, A. J. Marker III, K. Takeuchi, M. Smolley, and G. F. Ficini-Dorn, "Continuous Melting of Phosphate Laser Glasses," *J. Non-Cryst. Solids*, **263–264**, 342–57 (2000).

[10]F. Farges, D. R. Neuville, and G. E. Brown Jr., "Structural Investigation of Platinum Solubility in Silicate Glasses," *Am. Mineral.*, **84**, 1562–68 (1999).

[11]C. A. Click, R. K. Brow, P. R. Ehrmann, and J. H. Campbell, "Pt^{4+} Optical Absorption in Alumino-metaphosphate Laser Glasses," submitted to *J. Non-Cryst. Solids*.

[12]J. J. Bucher, N. M. Edelstein, K. P. Osborne, D. K. Shuh, N. Madden, P. Luke, D. Pehl, C. Cork, D. Malone, and P. G. Allen, "A Multichannel Monolithic Ge Detector System for Fluorescence X-ray Absorption Spectroscopy," *Rev. Sci. Instrum.*, **67** [9] 4 (1996).

[13]G. E. Brown Jr., G. Calas, G. Waychunas, and J. Petiau, "X-ray Absorption Spectroscopy and Its Applications in Mineralogy and Geochemistry," *Rev. Mineral.*, **18**, 431–512 (1988).

[14]B. K. Teo, *EXAFS: Basic Principles and Data Analysis*. Springer, Berlin, Germany, 1986.

[15]R. Prins and D. E. Koningsberger (eds.), *X-ray Absorption: Principles, Applications, Techniques of EXAFS, SEXAFS, and XANES*. Wiley-Interscience, New York, 1988.

[16]S. I. Zabinsky, J. J. Rehr, A. Ankudinov, R. C. Albers, and M. J. Eller, "Multiple-Scattering Calculations of X-ray-Absorption Spectra," *Phys. Rev. B*, **52** [4] 2995–3009 (1995).

[17]A. L. Ankudinov, J. J. Rehr, and S. R. Bare, "Hybridization Peaks in Pt–Cl XANES," *Chem. Phys. Let.*, **316** [5–6] 495–500 (2000).

[18]C. R. Natoli and M. Benfatto, "A Unifying Scheme of Interpretation of X-ray Absorption Spectra Based on the Multiple Scattering Theory," *J. Phys. (Paris)*, **47** [C-8] 11–23 (1986).

[19]S. Siegel, H. R. Hoekstra, and B. S. Tani, "The Crystal Structure of Beta-Platinum Dioxide," *J. Inorg. Nucl. Chem.*, **31** [12] 3803–807 (1969).

[20]M. T. Falqui, "The Crystal Structure of $PtCl_4$," *Ann. Chim. (Rome)*, **48**, 1160–67 (1958).

[21]R. J. Williams, D. R. Dillin, and W. O. Milligan, "Structure Refinement of Potassium Chloroplatinate by Powder and Single-Crystal Methods," *Acta Crystallogr. B*, **29** [7] 1369–72 (1973).

[22]A. W. Hull, "X-ray Crystal Analysis of Thirteen Common Metals," *Phys. Rev.*, **17**, 571–88 (1921).

[23]A. D. Westland; p. 12 in *Platinum-Group Elements: Mineralogy, Geology, Recovery*. Edited by L. J. Cabri. Canadian Institute of Mining and Metallurgy, Quebec, Canada, 1981.

[24]A. Paul and A. N. Tiwari, "Optical Absorption of Platinum(IV) in $Na_2O–B_2O_3$ and $Na_2O–NaCl–B_2O_3$ Glasses," *Phys. Chem. Glasses*, **14** [4] 69–72 (1973). □